Single-cell transcriptomic landscape of cardiac neural crest cell derivatives during embryonic and neonatal development

Xuanyu Liu, PhD[1]* Wen Chen, BSc[1]* Wenke Li, MSc[1] Ziyi Zeng, BSc[1]* James R. Priest, MD[2] Zhou Zhou, MD, PhD[1]

[1]State Key Laboratory of Cardiovascular Disease, Beijing Key Laboratory for Molecular Diagnostics of Cardiovascular Diseases, Center of Laboratory Medicine, Fuwai Hospital, National Center for Cardiovascular Diseases, Chinese Academy of Medical Sciences and Peking Union Medical College, Beijing 100037, China

[2]Stanford University School of Medicine, Stanford, CA 94305, USA

* X.L. and W.C. contributed equally to this manuscript

Running title: Single-cell RNA-seq of CNCC derivatives

Subject Terms:

Cell Biology /Structural Biology

Developmental Biology

Gene Expression and Regulation

Vascular Biology

Address correspondence to:

Dr. Zhou Zhou, e-mail: zhouzhou@fuwaihospital.org, No. 167, Beilishi Road, Xicheng District, Beijing, 100037, People's Republic of China

Word count: 7,159

ABSTRACT

Rationale: Cardiac neural crest cells (CNCCs) contribute greatly to cardiovascular development. A thorough understanding of the cell lineages, transcriptomic states and regulatory networks of CNCC derivatives during normal development is essential for deciphering the pathogenesis of CNCC-associated congenital anomalies. However, the transcriptomic landscape of CNCC derivatives during development has not yet been examined at a single-cell resolution.

Objective: We sought to systematically characterize the cell lineages, define the developmental chronology and elucidate the transcriptomic dynamics of CNCC derivatives during embryonic and neonatal development.

Methods and Results: We performed single-cell transcriptomic sequencing of 34,131 CNCC-derived cells in mouse hearts from eight developmental stages between E10.5 and P7. Through single-cell analyses and single-molecule fluorescence *in situ* hybridization, we confirmed the presence of CNCC-derived mural cells. Furthermore, we found the transition from CNCC-derived pericytes to microvascular smooth muscle cells, and identified the genes that were significantly regulated during this transition through pseudo-temporal analysis. CNCC-derived neurons first appeared at E10.5, which was earlier than previously recognized. In addition, the CNCC derivatives switched from a proliferative to a quiescent state with the progression of development. Gradual loss of the neural crest molecular signature with development was also observed in the CNCC derivatives. Our data suggested that many CNCC-derivatives had already committed or differentiated to a specific lineage when migrating to the heart. Finally, we characterized some previously unknown subpopulations of CNCC derivatives during development. For example, we found that *Penk*+ cells, which were mainly localized in outflow tract cushions, were all derived from CNCCs.

Conclusions: Our study provides novel insights into the cell lineages, molecular

signatures, developmental chronology and state change dynamics of CNCC derivatives during embryonic and neonatal development. Our dataset constitutes a valuable resource that will facilitate future efforts in exploring the role of CNCC derivatives in development and disease.

Key Words:

Single-cell RNA-seq, cardiac neural crest cell, cardiac mural cell, embryonic development, neonatal development

Nonstandard Abbreviations and Acronyms:

CCS	Cardiac conduction system
CNCC	Cardiac neural crest cell
GEM	Gel Beads-in-Emulsion
mVSMC	Microvascular smooth muscle cell
NCC	Neural crest cell
OFT	Outflow tract
PCA	Principal component analysis
smFISH	Single-molecule fluorescence in situ hybridization
TF	Transcriptional factor
UMAP	Uniform manifold approximation and projection
UMI	Unique molecular identifier
VSMC	Vascular smooth muscle cell

INTRODUCTION

Neural crest cells (NCCs) are a multipotent, migratory cell population that delaminates from the dorsal part of the neural tube via epithelial-to-mesenchymal transition.[1] During embryogenesis, migratory NCCs give rise to a plethora of cell lineages, and contribute to the development of a variety of tissues and organs, such as the skull bones, adrenal gland, enteric nervous system and heart.[2] While the heart is mostly of mesodermal origin, NCCs, which are ectodermal derivatives, contribute greatly to heart development.[3] The subpopulation of NCCs contributing to the heart are referred to as cardiac neural crest cells (CNCCs).[4] Since these cells were first discovered by Kirby et al.,[5] CNCCs have been demonstrated to play essential roles in cardiovascular development including the remodeling of the pharyngeal arch arteries, cardiac outflow tract (OFT) septation, valvulogenesis and cardiac innervation.[6] Genetic or environmental disturbance of the migration, survival and differentiation of CNCCs may result in congenital cardiovascular anomalies. Various human syndromes involving severe congenital heart defects have been associated with CNCCs, such as DiGeorge, Noonan and CHARGE syndromes.[4,6] A thorough understanding of the cell lineages, transcriptomic states and regulatory networks of CNCC derivatives during normal development is essential for deciphering the pathogenesis of these CNCC-associated congenital cardiovascular anomalies.

In recent decades, significant advances in understanding the CNCC contributions to heart development have been made by using lineage tracing mouse models such as *Wnt1-Cre* mice,[7] although some aspects remain contentious. In these models, all CNCCs and their derivatives are genetically labeled by the *Cre-loxP* recombinase system and observed via LacZ staining or fluorescence imaging (imaging-based lineage tracing).[8] After delamination from the neural tube (embryonic day 8.5, E8.5), CNCC derivatives first colonize the pharyngeal arch artery and ultimately differentiate into vascular smooth muscle cells (VSMCs) of the aortic arch.[4] Starting at E10.5, CNCC-

96 derived mesenchymal cells migrate into the OFT and join the cushion mesenchyme,
97 where they participate in the formation of the aorticopulmonary septum for complete
98 separation of the pulmonary and systemic circulation.[9] These CNCC-derived
99 mesenchymal cells eventually give rise to part of the smooth muscle walls of the great
100 arteries.[10] The remodeling of OFT cushions also result in the formation of semilunar
101 valvular leaflets, among which CNCC derivatives mainly contribute to the two leaflets
102 adjacent to the aorticopulmonary septum.[7,11] CNCCs have also been suggested to
103 directly contribute to the smooth muscle walls of the proximal coronary arteries.[7,12] In
104 addition to the entry point described above (i.e., the arterial pole of the heart), CNCC
105 derivatives enter the heart from a second entry point, the venous pole at E12.5, whereby
106 they penetrate the heart and migrate into the atrioventricular valves.[11,13] All the
107 melanocytes in atrioventricular valves are derived from CNCCs.[11]

108 In addition, neurons and glial cells derived from CNCCs contribute to the
109 parasympathetic innervation of the heart.[11,14] CNCC-derived neurons in the heart were
110 first observed at E11.5.[14,15] Although it has been suggested that CNCCs are required for
111 normal development of the cardiac conduction system (CCS), it remains contentious
112 whether CNCCs directly contribute to the CCS, which is known to be derived from the
113 myocardium (myocardial conducting cells).[4,6] Likewise, the presence of CNCC-derived
114 myocardial cells remains controversial, although it has been suggested that CNCCs are
115 essential for normal myocardial development.[4,16]

116 Mural cells include pericytes that discontinuously ensheath capillaries and
117 microvascular smooth muscle cells (mVSMCs) that cover larger-caliber vessels of the
118 microcirculation as well as their transitional cells.[17,18] Neural crest-derived mural cells
119 have been identified in various organs, such as the brain, retina, head and thymus.[19,20]
120 However, one previous study did not find any CNCC-derived mural cells in the heart
121 ventricle at E14.5 using lineage tracing.[21] Given that only one developmental stage was
122 examined in the previous study, it remains an open question whether CNCCs contribute

to cardiac mural cells.

It has become increasingly evident that even at the beginning of migration from the neural tube, the NCCs are heterogeneous, comprising multipotent cells, cells whose differentiation potential are restricted to varying degrees (fate-restricted cells), and even precursors committed to a particular lineage.[22] Although transcriptomic states have been investigated for pre-migratory or early migrating NCCs in the dorsal neural tube of the chick embryo,[23,24] little is known regarding the states of CNCC derivatives with respect to their differentiation potential and proliferative ability when they arrive at the heart or during embryonic and neonatal development of the heart.

One obvious drawback of imaging-based lineage tracing is that it cannot provide detailed molecular information about cell state transitions.[8] Recent technical advances in large-scale single-cell RNA-seq have enabled the transcriptomes of tens of thousands of cells to be assayed at a single-cell resolution.[25] As a complement to conventional imaging-based lineage tracing, large-scale single-cell RNA-seq allows unbiased cellular heterogeneity dissection, molecular signature identification and developmental trajectory reconstruction at an unprecedented scale and resolution. Large-scale time-series single-cell RNA-seq is becoming a powerful tool for studying the development of complex tissues, organs and even whole organisms.[26,27] However, to our knowledge, the transcriptomic landscape of CNCC derivatives during embryonic and neonatal development has not yet been examined at a single-cell resolution.

Here, we performed single-cell RNA-seq of CNCC derivatives in mouse hearts from eight developmental stages between E10.5 and P7 (postnatal day 7). We sought to systematically characterize the cell lineages, define the developmental chronology and elucidate the transcriptomic dynamics of CNCC derivatives during embryonic and neonatal development.

METHODS

The raw sequencing reads have been deposited in the Sequence Read Archive and are available through project accession number PRJNA562135. Detailed methods can be found in the Supplementary Methods.

RESULTS

Single-cell transcriptomic sequencing of CNCC derivatives during embryonic and neonatal development.

To investigate the transcriptomic landscape of CNCC derivatives during development, we used the *Wnt1-Cre;Rosa26-tdTomato* mouse model to specifically label CNCC-derived cells (Figure 1A). Whole hearts were dissociated, and *tdTomato*-positive cells were sorted for single-cell capture. The developmental stages we selected spanned from the very early time when CNCC derivatives arrived at the cardiac OFT during embryonic development (i.e., E10.5)[9] to neonatal stage P7 (Figure 1B). 10X Genomics Chromium Single Cell 3' transcriptomic sequencing libraries were constructed and subjected to sequencing. The sequencing quality metrics were similar across samples, reflecting relatively little technical variation (Online Table I). After the application of stringent quality control, we obtained high-quality single-cell transcriptomes of 34,131 CNCC-derived cells from eight stages. To facilitate further data exploration, we developed a web-based interface for our dataset (http://scrnaseqcncc.fwgenetics.org) that permits interactive examination of expression for any gene of interest.

The spatial distribution of the CNCC derivatives.

The visualization of *tdTomato*-positive cells by single-molecule fluorescence *in situ* hybridization (smFISH) enabled us to accurately obtain spatial distribution information for the CNCC derivatives, which was not included in the single-cell RNA-seq data (Figure 1C). At neonatal stage P7, we observed a large number of *tdTomato*-positive cells in the walls of the aorta and pulmonary artery (Figure 1C-D) as well as the aortic

and pulmonary valve leaflets (Figure 1E, Online Figure I), reflecting the great contribution of CNCCs to the OFT development. Notably, our smFISH results indicated that CNCC-derived cells only populated the inner medial cells of both the ascending aorta and aortic root (Figure 1C-D), thus supporting the view put forth in the most recent report about the distribution of CNCC- and SHF- derived VSMCs.[10] Consistent with previous reports,[7,11] the CNCC derivatives were found mainly in the two leaflets adjacent to the aorticopulmonary septum of aortic and pulmonary valves (i.e., right and left leaflets) (Online Figure I). Compared with the aortic and pulmonary valves (Figure 1E), the CNCCs made a much smaller contribution to the atrioventricular valves (Figure 1F). In addition, *tdTomato*-positive cells were found to be embedded in the walls of ventricles (Figure 1G). CNCC-derived VSMCs were observed in the coronary vasculature, as evidenced by the co-expression of *tdTomato* and a specific marker for mature VSMCs (i.e., *Myh11*) (Figure 1H).

Cell lineages and transcriptomic states of the CNCC derivatives during embryonic and neonatal development.

After recognizing the spatial distribution of the CNCC derivatives, we systematically dissected the cell lineages and transcriptomic states of the CNCC derivatives. The unsupervised clustering of the 34,131 CNCC-derived cells from eight stages identified 21 cell clusters (Figure 2A). The data structure was visualized in a two- or three-dimensional UMAP embedding (Online Data I). Six cell lineages were revealed by hierarchical clustering of the clusters based on the average expression of 2,000 selected features (Figure 2B) and the expression of established markers (Figure 2C). The representative molecular signatures for each cluster are shown in Figure 2D (Online Table II).

The VSMC (marked by the mature VSMC marker *Myh11*[28] and the immature VSMC marker *Cxcl12*[29]) and mesenchymal (marked by *Pdgfra*[30] and *Lum*[31]) lineages constituted the two largest lineages of the CNCC derivatives (accounting for 50.4% and

42.1% of the derivatives, respectively). Consistent with the differentiation of mesenchymal cells into VSMCs during development, these two lineages were aligned closely in the UMAP embedding (Figure 2A), and some intermediate subpopulations, such as c4, expressed markers of both lineages (Figure 2C). As expected, we identified CNCC-derived neurons (marked by the parasympathetic neuron marker *Slc18a3* and the sympathetic neuron marker *Th*[14]), Schwann cells (marked by *Gfra3* and *Cnp*[32]) and melanocytes (marked by *Mlana*[33] and *Dct*[34]). We did not find any CCS or myocardial cell clusters, so our data do not support a direct contribution of CNCCs to the CCS and myocardium in the mouse.

Intriguingly, we observed a cluster of mural cells (i.e., c19) based on the pericyte markers recently reported from single-cell studies: *P2ry14*[32] and *Vtn*[35] (Figure 2B-C), thus supporting the existence of CNCC-derived mural cells. To further confirm their mural cell identity, we examined the expression of canonical pericyte markers and VSMC contractile markers (Figure 2E). Compared with the others, the c19 cluster expressed higher levels of canonical pericyte markers including *Pdgfrb*, *Cspg4* (NG2), *Rgs5*, *Des* and *Kcnj8*.[18,36] It also exhibited high expression of VSMC contractile markers, including *Acta2*, *Cnn1* and *Myh11*,[28] reflecting a heterozygous microvascular mural population comprising both pericytes and mVSMCs. Our smFISH results ultimately validated the presence of CNCC-derived pericytes in the heart through the co-expression of *tdTomato* and *Vtn* (Figure 2F).

CNCC-derived pericytes transition to microvascular smooth muscle cells.

To understand the heterogeneity of the CNCC-derived mural cells, we performed subclustering of the c19 cells from stage P7 (227 cells, accounting for 48% of the cluster). Two subclusters were identified, sc1 and sc2, which correspond to pericytes and mVSMCs, respectively, based on the expression of markers (Figure 3A-B). RNA velocity analysis represents a computational framework that can infer the direction and rate of cellular state changes based on the relative abundance of spliced and unspliced

transcripts.[37] Our RNA velocity analysis revealed a transition from pericytes to mVSMCs, which is in agreement with a previous report that pericytes serve as progenitors for smooth muscle cells of the coronary vasculature.[38]

The single-cell data provided a unique opportunity for interrogating the regulatory changes during the transition. Pseudo-temporal ordering of the cells using Monocle2 resulted in the construction of a linear trajectory of cellular transition (Figure 3D-E). We further identified 952 genes that were significantly regulated during the progression of the transition (Figure 3F, Online Table III, adjusted P-value <1E-04). Hierarchical clustering of the identified genes revealed three clusters. Gene cluster I represented the molecular characteristics of pericytes and was mainly enriched for lysosomal membrane organization, cellular response to platelet-derived growth, cellular response to vascular endothelial growth factor stimulus and response to hypoxia (Figure 3F, Online Table IV). Gene cluster II reflected the phenotype of transitioning cells and was mainly enriched for mitochondrial electron transport, positive regulation of SMAD protein signal transduction, negative regulation of vascular smooth muscle cell proliferation and the response to fluid shear stress. Gene cluster III represented the characteristics of mVSMCs and was mainly enriched for positive regulation of transcription from RNA polymerase II promoter involved in smooth muscle cell differentiation and substrate adhesion-dependent cell spreading. Figure 3G shows the expression dynamics of the pericyte markers *Vtn* and *Pdgfrb* as well as the VSMC marker *Myh11*, reflecting a continuum of phenotypic changes in cells embedded in the walls of the microvasculature. Interestingly, Notch3 signaling has been suggested to be important in the pericyte to VSMC transition.[38] We found that *Notch3* was significantly up-regulated specifically in the middle phase of the trajectory (Figure 3G, adjusted P-value = 0.031), while other Notch receptors including *Notch1*, *Notch2* and *Notch4* were not significantly regulated. Moreover, we examined the transcription factors (TFs) that were significantly regulated during the transition (Figure 3H). Notably, *Fosb*, *Tbx2* and

Klf2 were specifically up-regulated in the middle phase of the trajectory, implying that they played roles in the transition.

Developmental chronology and transcriptomic state change dynamics of CNCC derivatives during development.

The study of the developmental chronology of CNCC derivatives has previously been limited by improper or limited cell markers for each developmental stage. The large-scale single-cell RNA-seq dataset gave us an unpreceded opportunity, since the cells were clustered in an unbiased manner based on the whole transcriptome, without the need for *a priori* knowledge about the cell markers. Figure 4A and 4B show the proportion of each cluster in each stage and the proportion of cells from each stage in each cluster, respectively. As shown in cluster I of Figure 4B, the melanocyte lineage first appeared at E11.5 and then greatly expanded at E14.5. These results are consistent with a previous report that *Dct* (a melanocyte marker) expression is first observed at E11.5 and that a larger number of melanocytes are found in the atrioventricular endocardial cushions at E14.5,[34] reflecting the reliability of our dataset. Surprisingly, CNCC-derived neurons were found to appear first at E10.5, which was earlier than previously recognized (E11.5).[13,14] Only six E10.5 neuron cells were captured, but they all expressed neural markers (Online Table V), thus excluding errors from data integration and clustering.

As expected, the VSMC lineage expanded mainly at the later stages of development (after E14.5; cluster II in Figure 4B), and the mesenchymal lineage expanded mainly at the early stages (before E14.5; cluster III in Figure 4B). Notably, the mural cells expanded greatly postnatally (especially at P7), in line with the increase in capillary growth during the postnatal development of the heart.[39] The transcriptomic state change dynamics during development of the CNCC-derived lineages can be clearly visualized in Figure 4C. Notably, the earliest sample from E10.5 included multiple cell lineages, supporting the view that many CNCC-derivatives had already committed or

differentiated to a specific lineage when they arrived at the heart.

Gradual loss of proliferation and the neural crest molecular signature with development in CNCC derivatives.

We further characterized the CNCC derivatives with respect to their proliferation ability and differentiation potential when they arrived at the heart as well as during embryonic and postnatal development. We found that the CNCC derivatives were highly proliferative when they arrived at the heart (E10.5) and switched from a proliferative to a quiescent state with the progression of development (Figure 5A). Some clusters, such as c18, c12, c8, c5 and c7, were highly proliferative (Figure 5B). We further investigated the differentiation potential of CNCC derivatives by examining the expression of a list of markers for pluripotency and pre-migratory neural crest cells that was compiled by a previous study.[23] No cell clusters were found to exhibit high expression of pluripotency genes such as *Nanog* and *Pou5f1* (*Oct4*), suggesting that the CNCC-derived cells generally did not possess stemness after migrating into the heart (Figure 5C). Moreover, we observed gradual loss of the neural crest molecular signature with development in the CNCC derivatives (Figure 5D). Notably, the CNCC-derived cell lineages exhibited differences in the neural crest molecular signature (Figure 5E). Surprisingly, the melanocytes, rather than the mesenchymal cells, were most similar to pre-migratory neural crest cells. The melanocytes also showed high expression of other neural crest markers, including *Pax3* and *Kit*[40] (Online Figure II).

Characterization of interesting cell subpopulations of CNCC derivatives during development.

Single-cell RNA-seq permits the identification of previously unrecognized subpopulations, and we characterized some interesting subpopulations that deserve further study. Cluster c1, c2 and c3 exhibited high expression of *Myh11*, thus representing relatively mature VSMCs (Figure 2C). However, c2 was aligned distant from c1 and c3 in the UMAP space (Figure 2A, Online Data I), suggesting that c2 represents another branch of the VSMC lineage distinct from c1 and c3, while the last

two clusters aligned together closely. Interestingly, compared with c1 and c3, c2 expressed significantly higher levels of contractile markers such as *Myh11* and *Cnn1* as well as pericyte markers such as *Rgs5* and *Kcnj8* (Figure 6A). Cluster c1 and c3 expressed significantly higher levels of extracellular matrix genes such as *Eln* and *Fbln2* than c2. Taken together, c2 may represent the CNCC-derived VSMCs of the coronary vasculature, while c1 and c3 may represent the CNCC-derived VSMCs of the great arteries. The smFISH results confirmed that the coronary arteries expressed significantly higher levels of *Myh11* than the great arteries (Figure 6B-C).

The mesenchymal cluster c11 showed high expression of the transcription factor *Tcf21* (Figure 6D), which may indicate a subpopulation of CNCC-derived valve interstitial cells based on the previous reports.[33,41] Our lab previously identified a *Penk*$^+$ mesenchymal subpopulation in the developing OFT; however, whether this subpopulation is derived from CNCCs was not answered.[29] In this study, we found the mesenchymal cluster c9 showed high expression of *Penk* (Figure 6E), and the smFISH results showed that the *Penk*$^+$ cells were mainly localized in the OFT cushions where the aortopulmonary septum formed, and all the *Penk*$^+$ cells were derived from CNCCs (Figure 6F).

Another interesting mesenchymal cluster is c5, which mainly comprised cells from the early stages (Figure 3A), suggesting that it may represent the early state of the CNCC-derived mesenchymal cells. This subpopulation showed high expression of the *Crabp1* gene, encoding cellular retinoic acid binding protein 1 (Figure 6G), which has been reported as the top marker of CNCC-derived mesenchymal cells at E9.25.[42] It also showed high expression of the *Crabp2* gene, encoding cellular retinoic acid binding protein 2 (Figure 6H). The expression of *Crabp1* and *Crabp2,* two important regulators of retinoic acid signaling, decreased during development. These results indicate that CNCC derivatives are more sensitive to retinoic acid signaling at early stages of development.

DISCUSSION

The neural crest is fascinating. The formation, migration and differentiation of NCCs and NCC-associated pathologies have been the subject of intense research since the discovery of these cells 150 years ago.[43] CNCCs play critical roles in the evolution and development of the vertebrate cardiovascular system.[44] In this study, we systematically investigated the transcriptional landscape of CNCC derivatives during cardiac development at a single-cell resolution. On the basis of large-scale single-cell RNA-seq analyses and smFISH validation, we reported the presence of CNCC-derived mural cells associated with the microvasculature. Furthermore, we found the transition from CNCC-derived pericytes to mVSMCs and identified the genes that were significantly regulated during the transition through pseudo-temporal ordering analysis. We defined the developmental chronology of the CNCC-derived lineages and found that the CNCC-derived neurons first appeared at E10.5, which was earlier than previously recognized. Our data indicated that many CNCC derivatives had already committed or differentiated to a specific lineage when they arrived at the heart. We found that the CNCC derivatives were highly proliferative when migrating into the heart, and switched from a proliferative to a quiescent state with the progression of development. Gradual loss of the neural crest molecular signature with development was also observed in the CNCC derivatives. The CNCC-derived cell lineages exhibited differences in the neural crest molecular signature. Surprisingly, the melanocytes were most similar to the pre-migratory neural crest cells. Finally, we confirmed some interesting subpopulations of the CNCC derivatives during development. For example, we found that *Penk*+ cells were mainly localized in the OFT cushions where the aortopulmonary septum formed, and confirmed that all the *Penk*+ cells were derived from CNCCs.

Understanding the origin and regulators driving the development of the cardiac vasculature is an important topic in developmental biology. Microvascular mural cells,

364 comprising microvascular pericytes and microvascular smooth muscle cells, have
365 recently been recognized playing a critical role in cardiac vascular homeostasis and
366 disease.[18] The plasticity of microvascular pericytes makes them promising cells for
367 application in cardiac regenerative medicine.[17] Nevertheless, the phenotypes of
368 microvascular mural cells are variable, and canonical markers such as *Pdgfrb*, *Des* and
369 *Cspg4* do not specifically label them, as also shown in our data (Figure 2E), thus
370 impeding the identification of the source and role of this important but heterogeneous
371 population of cells. Using lineage tracing and canonical markers, previous studies have
372 reported the embryonic origin of cardiac mural cells from epicardium or endocardial
373 endothelial cells.[21,45] Based on single-cell clustering and novel markers recently
374 reported from single-cell studies, we identified a third source of mural cells in the heart
375 (i.e., CNCC-derived mural cells) (Figure 2B-C). This finding makes sense because
376 NCCs have already been reported to give rise to mural cells in many organs, such as
377 the brain, retina and thymus.[19,20] We also found that the mural cells expanded greatly
378 postnatally (especially at P7, Figure 4B), in line with the increase in capillary growth
379 during the postnatal development of the heart.[39] This may be one of the reasons why
380 the CNCC-derived mural cells were not identified in a previous study[21] since the
381 CNCC-derived mural cells are relatively few at E14.5 (the stage that study only
382 examined). Consistent with the phenotypic heterogeneity of cardiac mural cells, our
383 results reflected a more complex embryonic origin of cardiac mural cells than
384 previously recognized. Whether cardiac mural cells of different origins behave
385 differentially during pathological processes of the coronary vasculature deserves further
386 study. Although a previous study indicated that pericytes can transition to mVSMCs,[38]
387 the gene expression dynamics underlying this transition are not yet fully elucidated.
388 Through pseudo-temporal ordering of single cells, we confirmed the linear trajectory
389 of the pericyte-to-mVSMC transition and, for the first time, elucidated the previously
390 unknown regulatory changes during the transition (Figure 3F). Our results support the
391 role of Notch3 signaling during the transition and provide candidate regulators

potentially driving the process (Figure 3H).

Although our data do not support a direct contribution of CNCCs to the CCS and myocardium, our results highlight the contribution of CNCCs to cardiac vessels of different calibers, from the VSMCs of the great arteries to mural cells wrapping the microvasculature. Moreover, we found that the phenotypes of the cells wrapping the cardiac vessels may vary as a function of the caliber of the vessels. For example, the coronary arteries expressed significantly higher levels of the contractile marker *Myh11* than the great arteries (Figure 6A-C). Our results reflect a continuum of cell phenotypes along the cardiac vascular tree with VSMCs and pericytes at the two ends of the phenotypic spectrum. The heterogeneity of the phenotypes of vessel-associated cells in the brain vasculature has been dissected using single-cell RNA-seq.[36] The phenotypic heterogeneity of the cardiac vasculature is also complex and deserves to be explored at a single-cell resolution in the future by integrating single-cell RNA-seq data with spatial transcriptomic data.[46]

Due to the limitations of imaging-based lineage tracing used in the previous studies,[7,11] we know little about the states of CNCC derivatives when they migrate to the heart or the molecular change dynamics during development. The large-scale single-cell RNA-seq dataset gave us unpreceded opportunity to explore these questions. Unexpectedly, CNCC-derived neurons expressing mature neuron markers were found to first appear at E10.5 (Figure 4B, Online Table V), which is earlier than previously recognized.[13,14] Notably, the earliest sample investigated from E10.5 contained multiple cell lineages and exhibited the expression of lineage-specific mature markers (Figure 4C). The neuron, Schwann and melanocyte lineages aligned relatively distant from the mesenchymal lineage in the UMAP embedding (Figure 4C), suggesting that most cells of these lineages were not differentiated from the mesenchymal lineage after migrating into the heart. No cell clusters were found to highly express the pluripotency genes such as *Nanog* and *Pou5f1*, suggesting that CNCC-derived cells generally do not possess

stemness after migrating into the heart (Figure 5C). Taken together, our results support the view that many CNCC-derivatives have already committed or differentiated to a specific lineage when they arrived at the heart. In addition, we observed that the CNCC derivatives were highly proliferative when migrating into the heart, and switched from a proliferative to a quiescent state with the progression of development (Figure 5A). We also observed gradual loss of the neural crest molecular signature with development in the CNCC derivatives. These findings revealed by single-cell analyses provide a deeper understanding of the CNCC derivatives during development.

In conclusion, our study provides novel insights into the cell lineages, molecular signatures, developmental chronology and state change dynamics of CNCC derivatives during embryonic and neonatal development. Our dataset constitutes a valuable resource that will facilitate future efforts to explore the roles of CNCC derivatives in development and disease.

AUTHOR CONTRIBUTIONS

X.L. performed data analysis, interpreted the results, and wrote the manuscript. W.C. performed the wet lab experiments with the assistance of Z. Zeng. W.L. designed the web interfaces. J. R. P. gave suggestions on result interpretation. Z. Zhou conceived the project. X.L. and W.C. participated in designing the project.

DISCLOSURES

There are no conflicts of interest to declare by any of the authors.

ACKNOWLEDGMENTS

We thank Dr. Zhen Zhang at Children's Hospital of Shanghai for transferring the Wnt1-Cre mouse line to our lab.

SOURCES OF FUNDING

This work is supported by grants from the National Natural Science Foundation of China (81900282), the CAMS Initiative for Innovative Medicine (2016-I2M-1-016), the Post-doctoral International Exchange Project (2018-BSH04), and the Foundation for Fuwai Hospital Youth Scholars (2019-F08).

REFERENCES

1. Bhatt S, Diaz R, Trainor PA. Signals and switches in mammalian neural crest cell differentiation. *Cold Spring Harb Perspect Biol*. 2013;5:a008326.

2. Szabo A, Mayor R. Mechanisms of neural crest migration. *Annu Rev Genet*. 2018;52:43–63.

3. Sieber-Blum M. Cardiac neural crest stem cells. *Anat Rec A Discov Mol Cell Evol Biol*. 2004;276:34–42.

4. Plein A, Fantin A, Ruhrberg C. Neural crest cells in cardiovascular development. *Curr Top Dev Biol*. 2015;111:183–200.

5. Kirby ML, Gale TF, Stewart DE. Neural crest cells contribute to normal aorticopulmonary septation. *Science (80-)*. 1983;220:1059–1061.

6. Keyte A, Hutson MR. The neural crest in cardiac congenital anomalies. *Differentiation*. 2012;84:25–40.

7. Jiang X, Rowitch DH, Soriano P, McMahon AP, Sucov HM. Fate of the mammalian cardiac neural crest. *Development*. 2000;127:1607–1616.

8. Wu SS, Lee JH, Koo BK. Lineage Tracing: computational reconstruction goes beyond the limit of imaging. *Mol Cells*. 2019;42:104–112.

9. Lin C-J, Lin C-Y, Chen C-H, Zhou B, Chang C-P. Partitioning the heart: mechanisms of cardiac septation and valve development. *Development*.

2012;139:3277–3299.

10. Sawada H, Rateri DL, Moorleghen JJ, Majesky MW, Daugherty A. Smooth muscle cells derived from second heart field and cardiac neural crest reside in spatially distinct domains in the media of the ascending aorta - brief report. *Arterioscler Thromb Vasc Biol*. 2017;37:1722–1726.

11. Nakamura T, Colbert MC, Robbins J. Neural crest cells retain multipotential characteristics in the developing valves and label the cardiac conduction system. *Circ Res*. 2006;98:1547–1554.

12. Arima Y, Miyagawa-Tomita S, Maeda K, Asai R, Seya D, Minoux M, Rijli FM, Nishiyama K, Kim KS, Uchijima Y, Ogawa H, Kurihara Y, Kurihara H. Preotic neural crest cells contribute to coronary artery smooth muscle involving endothelin signalling. *Nat Commun*. 2012;3:1267.

13. Poelmann RE, Jongbloed MRM, Molin DGM, Fekkes ML, Wang Z, Fishman GI, Doetschman T, Azhar M, Gittenberger-De Groot AC. The neural crest is contiguous with the cardiac conduction system in the mouse embryo: A role in induction? *Anat Embryol (Berl)*. 2004;208:389–393.

14. Hildreth V, Webb S, Bradshaw L, Brown NA, Anderson RH, Henderson DJ. Cells migrating from the neural crest contribute to the innervation of the venous pole of the heart. *J Anat*. 2008;212:1–11.

15. Végh A, Duim S, Smits A, Poelmann R, ten Harkel A, DeRuiter M, Goumans M, Jongbloed M. Part and Parcel of the Cardiac Autonomic Nerve System: Unravelling Its Cellular Building Blocks during Development. *J Cardiovasc Dev Dis*. 2016;3:28.

16. Engleka KA, Gitler AD, Zhang M, Zhou DD, High FA, Epstein JA. Insertion of Cre into the Pax3 locus creates a new allele of Splotch and identifies

491 unexpected Pax3 derivatives. *Dev Biol*. 2005;280:396–406.

492 17. Avolio E, Madeddu P. Discovering cardiac pericyte biology: From
493 physiopathological mechanisms to potential therapeutic applications in
494 ischemic heart disease. *Vasc Pharmacol*. 2016;86:53–63.

495 18. Holm A, Heumann T, Augustin HG. Microvascular mural cell organotypic
496 heterogeneity and functional plasticity. *Trends Cell Biol*. 2018;28:302–316.

497 19. Zachariah MA, Cyster JG. Neural crest-derived pericytes promote egress of
498 mature thymocytes at the corticomedullary junction. *Science (80-)*.
499 2010;328:1129–1135.

500 20. Trost A, Schroedl F, Lange S, Rivera FJ, Tempfer H, Korntner S, Stolt CC,
501 Wegner M, Bogner B, Kaser-Eichberger A, Krefft K, Runge C, Aigner L,
502 Reitsamer HA. Neural crest origin of retinal and choroidal pericytes. *Investig*
503 *Ophthalmol Vis Sci*. 2013;54:7910–7921.

504 21. Chen Q, Zhang H, Liu Y, Adams S, Eilken H, Stehling M, Corada M, Dejana
505 E, Zhou B, Adams RH. Endothelial cells are progenitors of cardiac pericytes
506 and vascular smooth muscle cells. *Nat Commun*. 2016;7:12422.

507 22. Kalcheim C. Neural crest cells and their derivatives. In: Encyclopedic
508 Reference of Genomics and Proteomics in Molecular Medicine. Berlin,
509 Heidelberg: Springer Berlin Heidelberg; 2006. p. 1254–1258.

510 23. Lignell A, Kerosuo L, Streichan SJ, Cai L, Bronner ME. Identification of a
511 neural crest stem cell niche by Spatial Genomic Analysis. *Nat Commun*.
512 2017;8:1830.

513 24. Tani-Matsuhana S, Vieceli FM, Gandhi S, Inoue K, Bronner ME.
514 Transcriptome profiling of the cardiac neural crest reveals a critical role for
515 MafB. *Dev Biol*. 2018;

516 25. Zheng GX, Terry JM, Belgrader P, Ryvkin P, Bent ZW, Wilson R, Ziraldo SB,
517 Wheeler TD, McDermott GP, Zhu J, Gregory MT, Shuga J, Montesclaros L,
518 Underwood JG, Masquelier DA, Nishimura SY, Schnall-Levin M, Wyatt PW,
519 Hindson CM, Bharadwaj R, Wong A, Ness KD, Beppu LW, Deeg HJ,
520 McFarland C, Loeb KR, Valente WJ, Ericson NG, Stevens EA, Radich JP,
521 Mikkelsen TS, Hindson BJ, Bielas JH. Massively parallel digital transcriptional
522 profiling of single cells. *Nat Commun*. 2017;8:14049.

523 26. Plass M, Solana J, Wolf FA, Ayoub S, Misios A, Glažar P, Obermayer B,
524 Theis FJ, Kocks C, Rajewsky N. Cell type atlas and lineage tree of a whole
525 complex animal by single-cell transcriptomics. *Science (80-).*
526 2018;360:eaaq1723.

527 27. Cao J, Spielmann M, Qiu X, Huang X, Ibrahim DM, Hill AJ, Zhang F,
528 Mundlos S, Christiansen L, Steemers FJ, Trapnell C, Shendure J. The single-
529 cell transcriptional landscape of mammalian organogenesis. *Nature*.
530 2019;566:496–502.

531 28. Sinha S, Iyer D, Granata A. Embryonic origins of human vascular smooth
532 muscle cells: implications for in vitro modeling and clinical application. *Cell*
533 *Mol Life Sci*. 2014;71:2271–2288.

534 29. Liu X, Chen W, Li W, Li Y, Priest JR, Zhou B, Wang J, Zhou Z. Single-cell
535 RNA-seq of the developing cardiac outflow tract reveals convergent
536 development of the vascular smooth muscle cells. *Cell Rep*. 2019;28:1346-
537 1361.e4.

538 30. Farahani RM, Xaymardan M. Platelet-derived growth factor receptor alpha as a
539 marker of mesenchymal stem cells in development and stem cell biology. *Stem*
540 *Cells Int*. 2015;2015:8.

541 31. Camp JG, Badsha F, Florio M, Kanton S, Gerber T, Wilsch-Bräuninger M,

Lewitus E, Sykes A, Hevers W, Lancaster M, Knoblich JA, Lachmann R, Pääbo S, Huttner WB, Treutlein B. Human cerebral organoids recapitulate gene expression programs of fetal neocortex development. *Proc Natl Acad Sci U S A*. 2015;112:15672–15677.

32. Skelly DA, Squiers GT, McLellan MA, Bolisetty MT, Robson P, Rosenthal NA, Pinto AR. Single-Cell Transcriptional Profiling Reveals Cellular Diversity and Intercommunication in the Mouse Heart. *Cell Rep*. 2018;22:600–610.

33. Hulin A, Hortells L, Gomez-Stallons MV, O'Donnell A, Chetal K, Adam M, Lancellotti P, Oury C, Potter SS, Salomonis N, Yutzey KE. Maturation of heart valve cell populations during postnatal remodeling. *Development*. 2019;146:dev173047.

34. Brito FC, Kos L. Timeline and distribution of melanocyte precursors in the mouse heart. *Pigment Cell Melanoma Res*. 2008;21:464–470.

35. Farbehi N, Patrick R, Dorison A, Xaymardan M, Janbandhu V, Wystub-Lis K, Ho JW, Nordon RE, Harvey RP. Single-cell expression profiling reveals dynamic flux of cardiac stromal, vascular and immune cells in health and injury. *Elife*. 2019;8:e43882.

36. Vanlandewijck M, He L, Mäe MA, Andrae J, Ando K, Del Gaudio F, Nahar K, Lebouvier T, Laviña B, Gouveia L, Sun Y, Raschperger E, Räsänen M, Zarb Y, Mochizuki N, Keller A, Lendahl U, Betsholtz C. A molecular atlas of cell types and zonation in the brain vasculature. *Nature*. 2018;554:475–480.

37. La Manno G, Soldatov R, Zeisel A, Braun E, Hochgerner H, Petukhov V, Lidschreiber K, Kastriti ME, Lönnerberg P, Furlan A, Fan J, Borm LE, Liu Z, van Bruggen D, Guo J, He X, Barker R, Sundström E, Castelo-Branco G, Cramer P, Adameyko I, Linnarsson S, Kharchenko P V. RNA velocity of single cells. *Nature*. 2018;560:494–498.

568 38. Volz KS, Jacobs AH, Chen HI, Poduri A, McKay AS, Riordan DP, Kofler N,
569 Kitajewski J, Weissman I, Red-Horse K. Pericytes are progenitors for coronary
570 artery smooth muscle. *Elife*. 2015;4:e10036.

571 39. Riley PR, Smart N. Vascularizing the heart. *Cardiovasc Res*. 2011;91:260–268.

572 40. Hatzistergos KE, Takeuchi LM, Saur D, Seidler B, Dymecki SM, Mai JJ,
573 White IA, Balkan W, Kanashiro-Takeuchi RM, Schally A V., Hare JM. cKit+
574 cardiac progenitors of neural crest origin. *Proc Natl Acad Sci*.
575 2015;112:13051–13056.

576 41. Acharya A, Baek ST, Banfi S, Eskiocak B, Tallquist MD. Efficient inducible
577 Cre-mediated recombination in Tcf21 cell lineages in the heart and kidney.
578 *Genesis*. 2011;49:870–877.

579 42. Soysa TY de, Ranade S, Okawa S, Ravichandran S, Huang Y, Salunga H,
580 Schricker A, Sol A del, Gifford C, Srivastava D. Single-cell transcriptome
581 analysis during cardiogenesis reveals basis for organ level developmental
582 anomalies. *Nature*. 2019;572:120–124.

583 43. Prasad MS, Charney RM, García-Castro MI. Specification and formation of the
584 neural crest: Perspectives on lineage segregation. *Genesis*. 2019;57:1–21.

585 44. Keyte AL, Alonzo-Johnsen M, Hutson MR. Evolutionary and developmental
586 origins of the cardiac neural crest: Building a divided outflow tract. *Birth*
587 *Defects Res Part C - Embryo Today Rev*. 2014;102:309–323.

588 45. Zhou B, Ma Q, Rajagopal S, Wu SM, Domian I, Rivera-Feliciano J, Jiang D,
589 Von Gise A, Ikeda S, Chien KR, Pu WT. Epicardial progenitors contribute to
590 the cardiomyocyte lineage in the developing heart. *Nature*. 2008;454:109–113.

591 46. Moncada R, Wagner F, Chiodin M, Devlin JC, Baron M, Hajdu CH, Simeone
592 DM, Yanai I. Integrating single-cell RNA-Seq with spatial transcriptomics in

593 pancreatic ductal adenocarcinoma using multimodal intersection analysis.

594 *bioRxiv*. 2019;

595

596 **FIGURES WITH FIGURE LEGENDS**

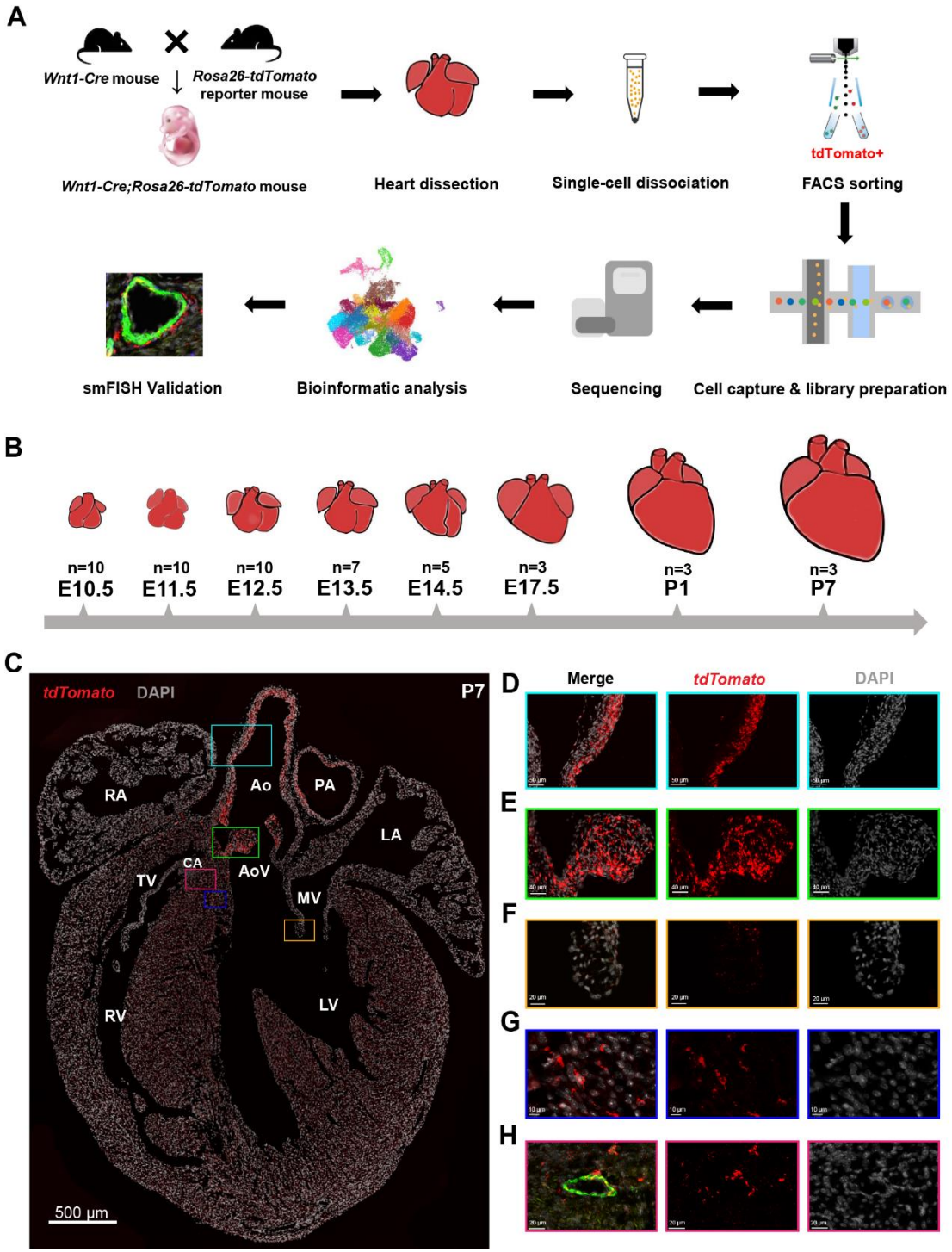

597

598 **Figure 1. Single-cell RNA-seq and spatial distribution of the CNCC derivatives.**

599 **(A)** Schematic representation of the experimental procedure. **(B)** The developmental

600 stages at which the hearts were sampled. Multiple hearts were pooled as a sample for
601 each stage. **(C)** The spatial distribution of the CNCC derivatives labeled by *tdTomato*.
602 **(D-H)** Magnified views of the rectangular regions in C. The same regions are indicated
603 by the same colors. In H, the vessel wall is indicated by the green fluorescence of the
604 VSMC marker *Myh11*. Ao, aorta; AoV, aortic valve; CA, coronary artery; LA, left
605 atrium; LV, left ventricle; MV, mitral valve; PA, pulmonary artery; RA, right atrium;
606 RV, right ventricle; TV, tricuspid valve

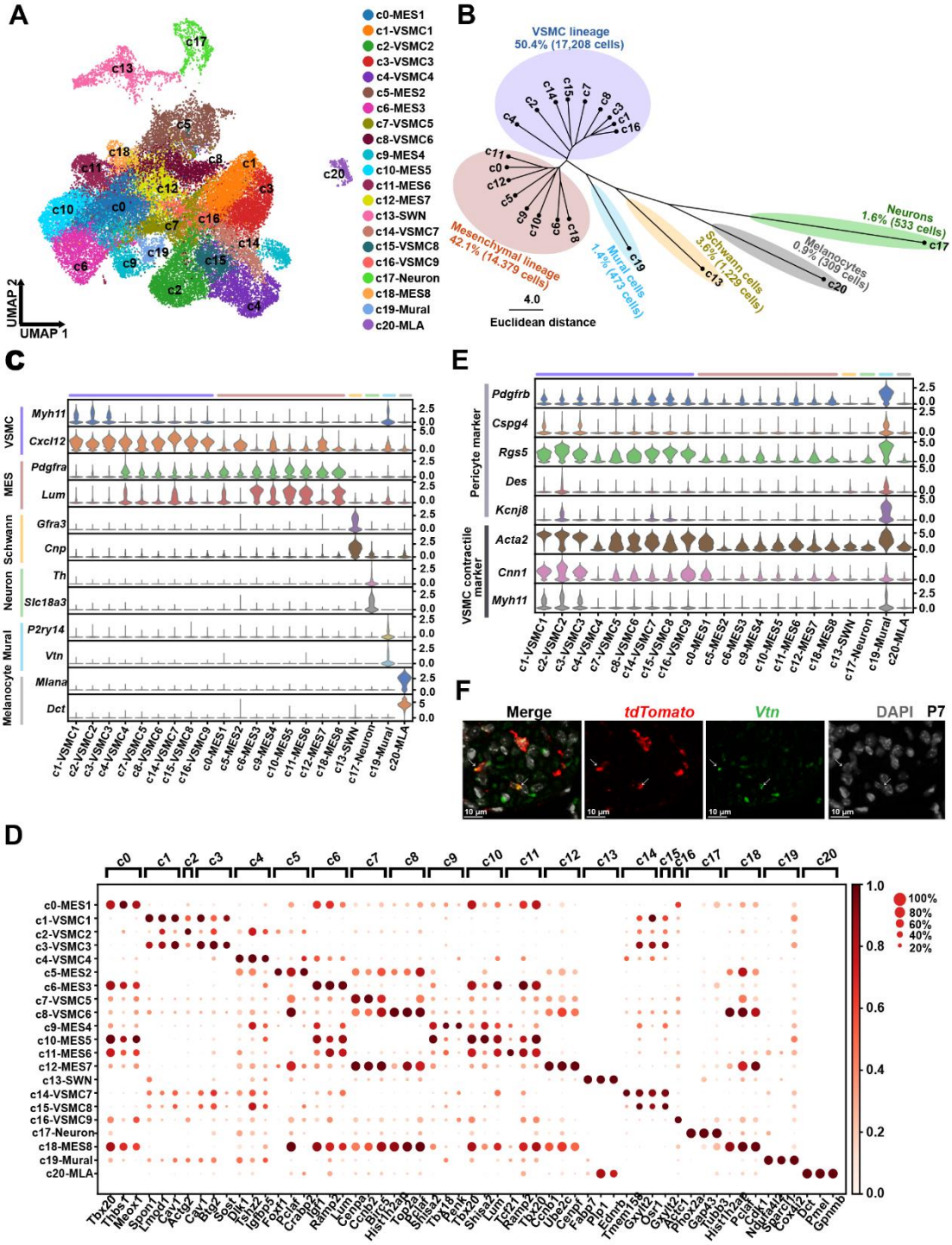

607

608 **Figure 2. Cell lineages and transcriptomic states of CNCC derivatives during**
609 **embryonic and neonatal development. (A)** Single-cell transcriptomes of 34,131
610 CNCC derivatives projected on a two-dimensional UMAP embedding. Clusters are

611 distinguished by different colors. **(B)** Hierarchical clustering of the clusters based on
612 the average expression of 2,000 selected features. **(C)** Expression of established
613 markers for each cell lineage in each cluster. **(D)** Representative molecular signatures
614 for each cluster. The area of the circles denotes the proportion of cells expressing the
615 gene, and the color intensity reflects the expression intensity. **(E)** Expression of
616 canonical pericyte markers and VSMC contractile markers. **(F)** smFISH validation of
617 CNCC-derived pericytes. Hearts from P7 mice were used. Arrows indicate the co-
618 expression of *tdTomato* and the pericyte marker *Vtn*. MES, mesenchymal cell; MLA,
619 melanocyte; SWN, Schwann cell; UMAP, uniform manifold approximation and
620 projection; VSMC, vascular smooth muscle cell

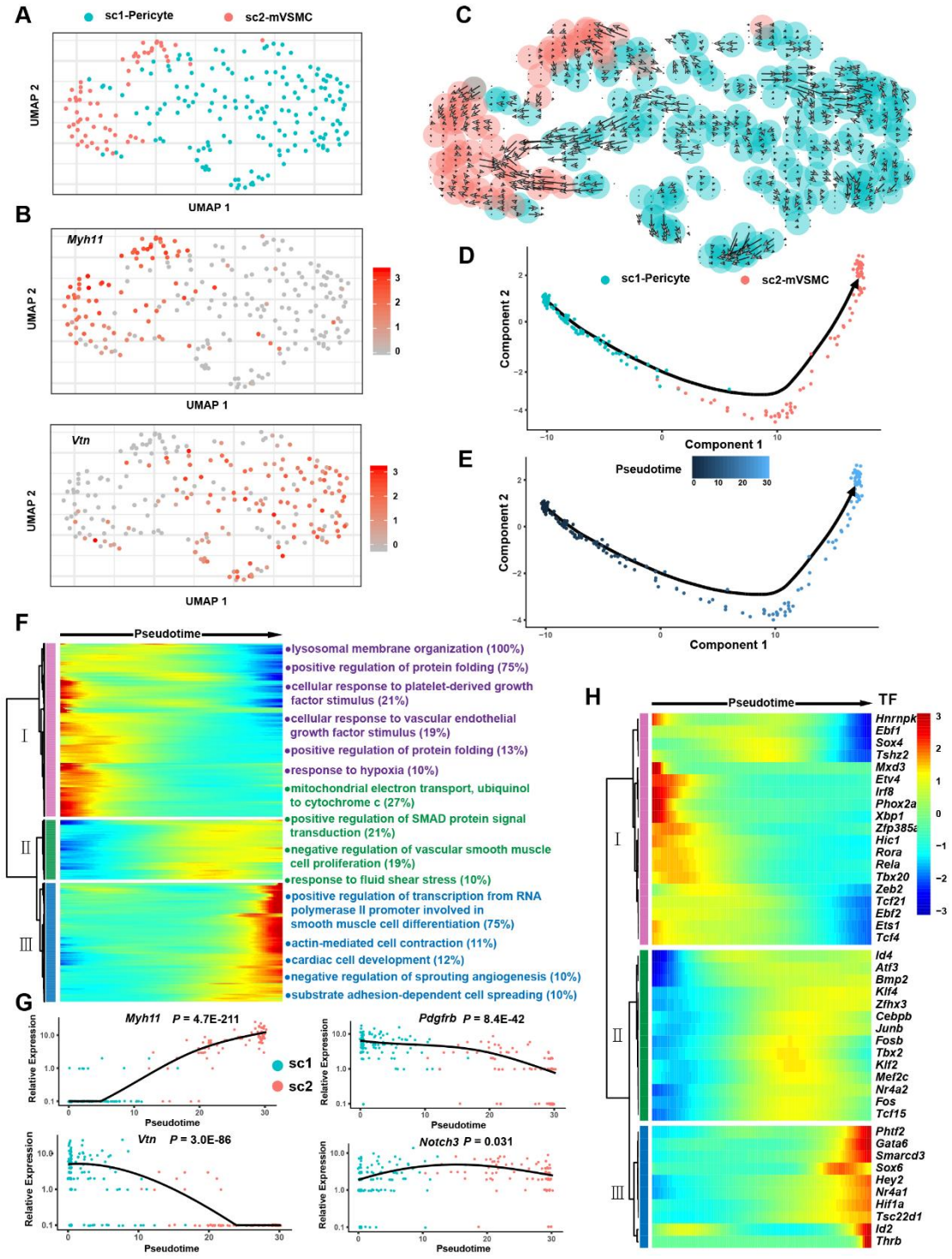

Figure 3. Cellular transition from CNCC-derived pericytes to microvascular smooth muscle cells. (A) Subclustering of the mural cell cluster c19 reveals two subpopulations. mVSMC, microvascular smooth muscle cells. Only P7 cells were

625 considered in this analysis. **(B)** The expression distribution of the VSMC-specific
626 marker *Myh11* and the pericyte marker *Vtn*. **(C)** RNA velocity analysis reveals a
627 transition from CNCC-derived pericytes to mVSMCs. The direction and length of the
628 arrow reflect the direction and rate of cellular state changes, respectively. **(D)** Linear
629 trajectory constructed via pseudo-temporal ordering of cells. **(E)** Transition trajectory
630 colored according to pseudotime. **(F)** Hierarchical clustering of the genes that were
631 significantly regulated during the progression of the transition. Only genes with an
632 adjusted P-value <1E-04 are shown here. The number in the parentheses represents the
633 percentage of genes associated with the Gene Ontology term for which the gene cluster
634 is significantly enriched (adjusted P-value <0.05). **(G)** The expression changes in
635 *Myh11*, *Vtn*, *Pdgfrb* and *Notch3* during the progression of the cellular transition. **(H)**
636 Transcriptional factors that were significantly regulated during the transition.

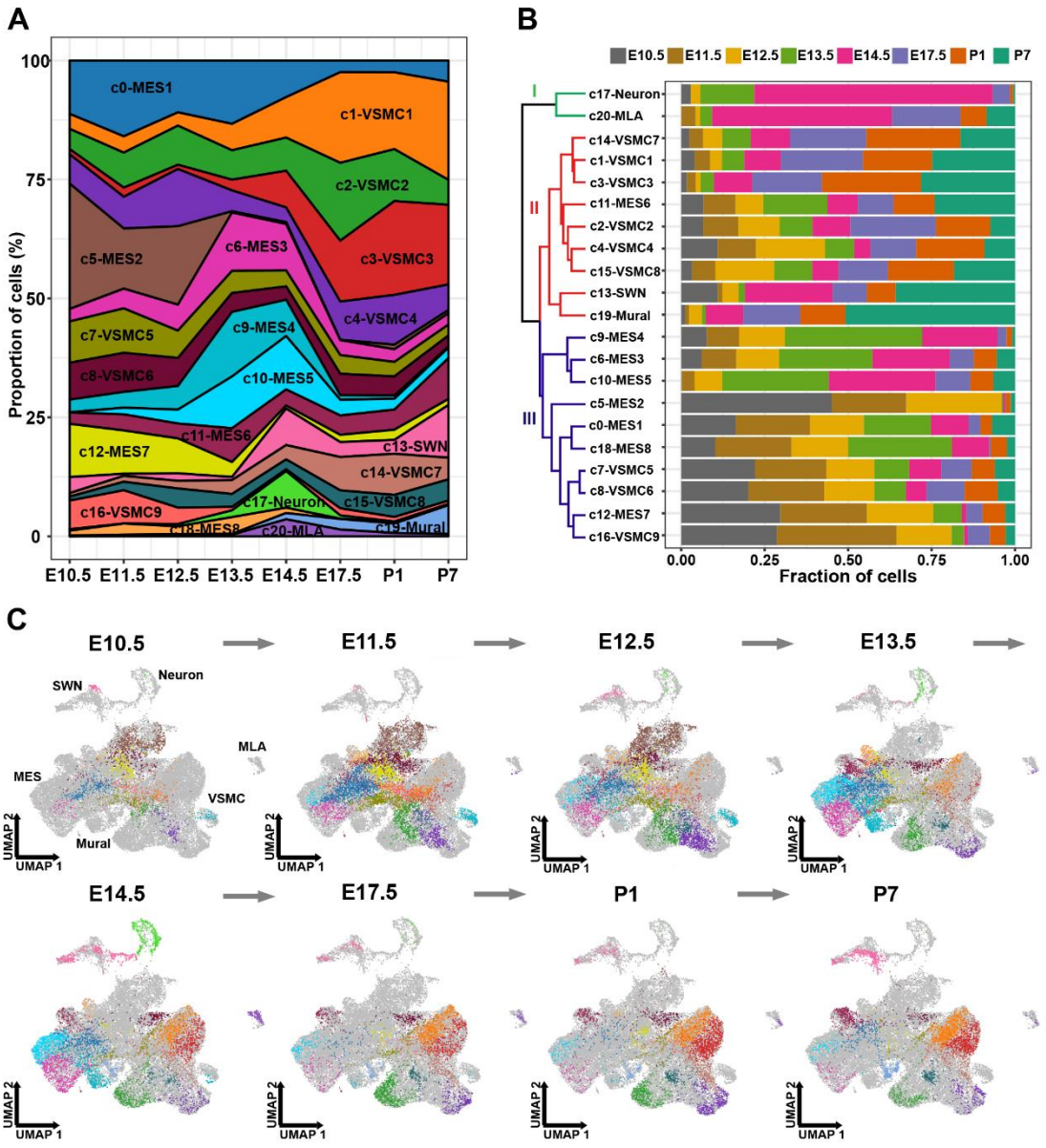

637

638 **Figure 4. The developmental chronology and transcriptomic state change**
639 **dynamics of CNCC derivatives. (A)** The proportion of cells of each cluster in each
640 stage. **(B)** The proportion of cells from each stage in each cluster. All samples are
641 normalized to the same number of cells (2,026). The dendrogram shows the hierarchical
642 clustering of the cell clusters based on the proportion of cells from each stage. **(C)**
643 Dynamic changes in the transcriptomic states of CNCC derivatives during development.
644 The cells are colored according to the clusters. MES, mesenchymal cell; MLA,
645 melanocyte; SWN, Schwann cell; UMAP, uniform manifold approximation and

646 projection; VSMC, vascular smooth muscle cell

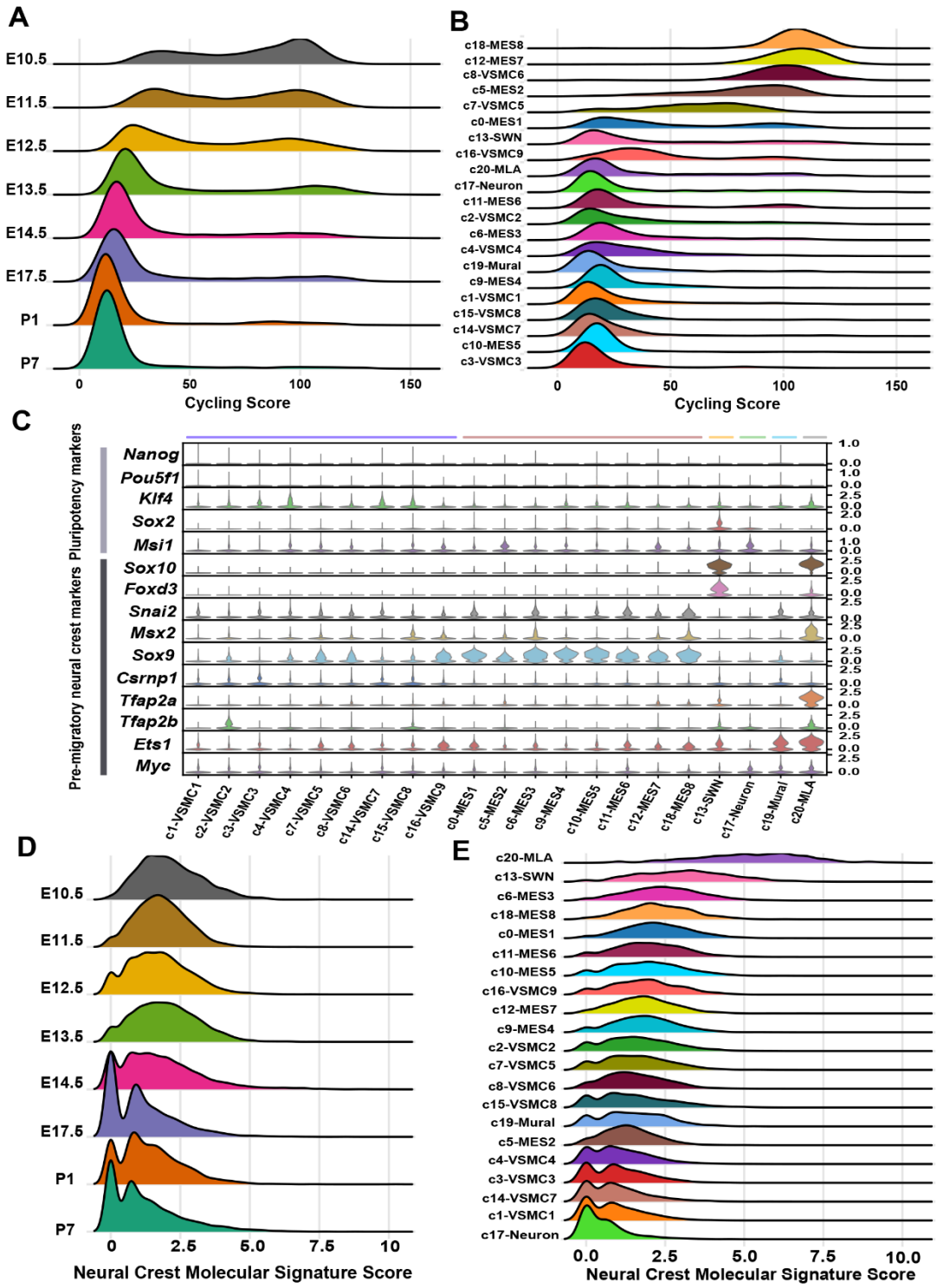

647

648 **Figure 5. Gradually loss of proliferation and the neural crest molecular signature**

649 **with development in the CNCC derivatives. (A)** Ridge plot showing that CNCC

650 derivatives switched from a proliferative to a quiescent state with the progression of
651 development. The cycling score of each cell was calculated by summing the log-
652 normalized expression of the cycling genes ("g2m.genes" and "s.genes" in Seurat).
653 **(B)** Ridge plot showing the proliferative ability of each cell cluster. **(C)** The expression
654 of pluripotency and pre-migratory neural crest markers in each cell cluster. **(D)** Ridge
655 plot showing that the divergence in molecular signatures between the CNCC derivatives
656 and pre-migratory neural crest cells increased during development. The neural crest
657 molecular signature score was calculated by summing the log-normalized expression
658 of the pre-migratory neural crest markers (shown in C). **(E)** Ridge plot showing the
659 distribution of the neural crest molecular signature score in each cluster.

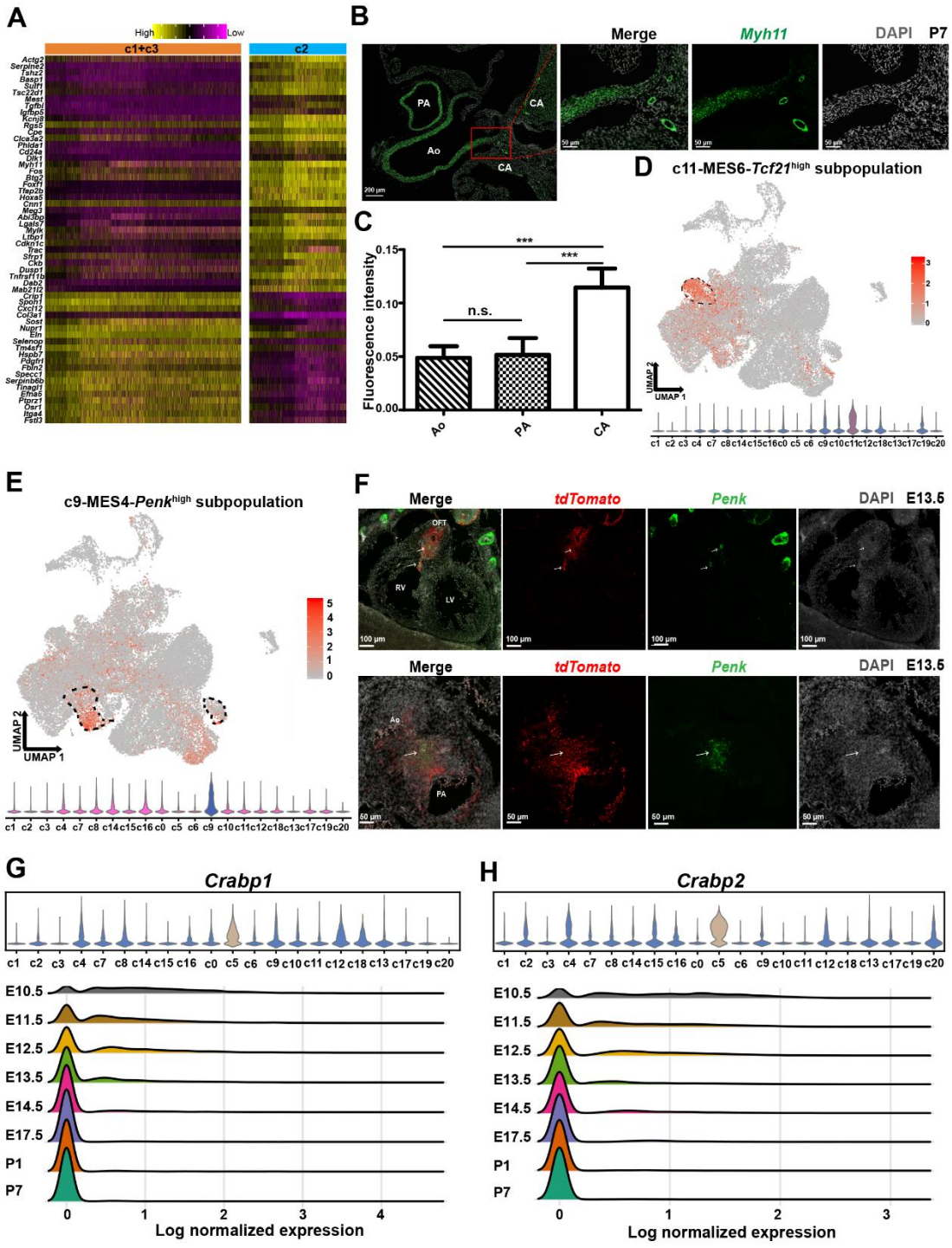

660

661 **Figure 6. Characterization of interesting cell subpopulations of CNCC derivatives**
662 **during development. (A)** Heatmap showing the difference between VSMC clusters c2
663 and c1+c3. The significance threshold was set to an adjusted P-value < 0.05 and log2-
664 fold change > 0.25. **(B)** smFISH results showing significantly higher expression of the

665 contractile marker *Myh11* in VSMCs of the coronary arteries than in VSMCs of the
666 great arteries. **(C)** Quantitative analysis of the fluorescent intensity of *Myh11* expression
667 confirms significantly higher expression of *Myh11* in VSMCs of the coronary arteries
668 than in VSMCs of the great arteries. The bar height represents the average intensity of
669 five biological replicates (±SE). One-way ANOVA with Turkey's post-hoc test. P-
670 value ≤ 0.001 (***). n.s. not significant. **(D)** Mesenchymal cluster c11 with high *Tcf21*
671 expression may represent valve interstitial cells. **(E)** Mesenchymal cluster c9 shows
672 high expression of *Penk*. **(F)** smFISH results showing that the *Penk*+ cells are mainly
673 localized in the OFT region and are derived from CNCC. **(G)** *Crabp1* shows high
674 expression in mesenchymal cluster c5 and its expression decreases with development.
675 **(H)** *Crabp2* shows high expression in mesenchymal cluster c5 and its expression
676 decreases with development. Ao, aorta; CA coronary artery; LV, left ventricle; OFT,
677 outflow tract; PA, pulmonary artery; RV, right ventricle.